AMPK Activation by 5-Amino-4-Imidazole Carboxamide Riboside-1-β-D-Ribofuranoside Attenuates Alkali Injury-Induced Corneal Fibrosis

Selikem Abla Nuwormegbe[1] and Sun Woong Kim[2]

[1]Department of Global Medical Science, Wonju College of Medicine, Yonsei University, Wonju-si, Gangwon-do, Republic of Korea
[2]Department of Ophthalmology, Wonju College of Medicine, Yonsei University, Wonju-si, Gangwon-do, Republic of Korea

PURPOSE. Increased TGF-β1 synthesis after corneal alkali injury is implicated in corneal fibrosis, as it promotes transdifferentiation of keratocytes into myofibroblasts. The activation of 5′-adenosine monophosphate-activated protein kinase (AMPK) by 5-amino-4-imidazole carboxamide riboside-1-β-D-ribofuranoside (AICAR) inhibits TGF-β1-induced fibrosis in other cell types. We investigated the antifibrotic effect of AICAR in corneal fibroblasts after alkali injury.

METHODS. Mouse models of corneal alkali burn, produced by placing 2-mm-diameter filter paper soaked in 0.1-N NaOH on the right cornea for 30 seconds, were treated with the test drugs 4× daily for 21 days. The central cornea was scanned by optical coherence tomography (OCT). Corneal tissues were obtained and processed for western blotting and immunohistochemistry. For in vitro analysis, primary human corneal fibroblasts were treated directly with TGF-β1 to induce fibrosis, with or without AICAR pretreatment. Myofibroblast activation and extracellular matrix (ECM) protein synthesis were detected by western blotting, real-time PCR, and collagen gel contraction assay. Signaling proteins were analyzed by western blotting.

RESULTS. Alkali injury induced the upregulation of TGF-β1 expression, which led to increased α-smooth muscle actin (α-SMA) and fibronectin synthesis and myofibroblast differentiation. AMPK activation by AICAR significantly suppressed TGF-β1 and ECM protein expression. The antifibrotic effect of AICAR was AMPK dependent, as treatment with the AMPK inhibitor Compound C attenuated the antifibrotic response.

CONCLUSIONS. AMPK activation by AICAR suppresses the myofibroblast differentiation and ECM synthesis that occur after alkali injury in corneal fibroblasts.

Keywords: AMPK, AICAR, alkali burn, corneal fibroblasts, fibrosis

Cornea alkali burn is caused by exposure of the eye to alkaline substances. The pH, degree of contact, and duration of exposure determine the severity of the injury.[1,2] The strong alkali causes tissue saponification. The damaged tissues then undergo liquefactive necrosis, causing an inflammatory response that leads to the release of proteolytic enzymes that further damage the tissues.[2–5]

Research indicates that increased synthesis of TGF-β1 following corneal alkali injury helps the healing process. It promotes the migration of keratocytes and epithelial cells to the site of the injury, causes chemotaxis of monocytes and macrophages, and induces myofibroblasts transdifferentiation.[6–8] However, its overexpression induces the expression of vascular endothelial growth factor (VEGF) and monocyte/macrophage chemotactic protein-1 (MCP-1),[9,10] which cause local neovascularization and inflammation, respectively,[11–14] resulting in fibrosis. Preventing the overexpression of TGF-β1 and its downstream signaling effects is thus critical in preventing fibrosis.

5′-Adenosine monophosphate-activated protein kinase (AMPK) is a cellular energy sensor that is activated by an increased intracellular AMP/adenosine triphosphate (ATP) ratio.[15] It is also activated by AMP/ATP ratio-independent pathways, such as the Ca^{2+}/calmodulin-dependent protein kinase.[16] In addition to these physiological conditions, AMPK is activated by pharmacological agents such as 5-amino-4-imidazole carboxamide riboside-1-β-D-ribofuranoside (AICAR), which is an adenosine analog. AICAR is taken up into the cells by adenosine transporters on the cell membrane and subsequently phosphorylated by adenosine kinase to 5-amino-1-β-D-ribofuranosylimidazole-4-carboxamide-5′-monophosphate (ZMP), which mimics AMP and thus stimulates AMPK activation.[17,18] AMPK activation has several effects, including modulation of protein synthesis, glucose and lipid metabolism, regulation of cytokine production and inflammation, and cellular proliferation and apoptosis.[19–22] In addition, the activation of AMPK by AICAR has been shown to exhibit antifibrotic effects

in several cell types,[23–27] making it a potential therapeutic agent in countering fibrosis. Its role in corneal fibrosis, however, has yet to be investigated. This study focused on the antifibrotic effect of AICAR in the cornea and the molecular mechanisms involved.

METHODS

Ethical Statement

The animal study was approved by the Yonsei University Wonju College of Medicine (YWC-170410-1). All of the experiments were carried out in accordance with the guidelines issued by the Animal Care and Ethics Committee on Research at Yonsei University Wonju College of Medicine, in accordance with the tenets of the Helsinki Declaration, and conducted with adherence to the ARVO Statement for the Use of Animals in Ophthalmic and Vision Research.

Isolation and Culture of Primary Human Cornea Fibroblasts

Primary human corneal fibroblasts were obtained from the corneal limbus after removal of the central corneal buttons for corneal transplantation. Briefly, the other cornea layers, including the epithelium and endothelium, were removed with Dispase II digestion (Sigma-Aldrich, St. Louis, MO, USA) and scraping under a microscope. The stromal layer was then washed three times with sterile PBS (Welgene, Gyeongsan, Korea), and the tissue was digested with 2 mg/mL collagenase and 0.5 mg/mL hyaluronidase (Sigma-Aldrich) prepared in Dulbecco's Modified Eagle Medium/Nutrient Mixture F12 (DMEM/F12) (Thermo Fisher Scientific, Waltham, MA, USA) medium for 3 hours with shaking at 37°C. After digestion, the isolated cells were collected by centrifugation (12000×g for 5 minutes), resuspended in DMEM/F12 supplemented with 10% fetal bovine serum (FBS) and 1% antibiotic/antimycotic (Thermo Fisher Scientific), and incubated at 37°C with 5% CO_2 in a humidified incubator.[28] The cells were passaged with 0.25% trypsin and cultured in DMEM supplemented with 5% FBS and 1% antibiotic/antimycotic. The culture medium was changed every 2 to 3 days until passaging at 80% confluency. The cells at passages 3 to 10 were stored at –80°C for subsequent use.

In Vitro Analyses

In vitro analyses were performed by directly stimulating primary corneal fibroblasts with TGF-β1 to induce fibrosis. The fibroblasts were seeded into culture plates and allowed to attach. The cells were pretreated with 0.5-mM and 1-mM AICAR (Abcam, Cambridge, UK) dissolved in dimethyl sulfoxide for 2 to 3 hours followed by 5 ng/mL TGF-β1 (PeproTech, Seoul, Korea) and then incubated. To determine if the observed effects were AMP-activated protein kinase (AMPK) dependent, the cells were pretreated for 2 hours with 2.5-μM and 5-μM Compound C (Merck, Darmstadt, Germany), an AMPK antagonist, followed by 1-mM AICAR for 2 hours and then 5-ng/mL TGF-β1, and then incubated. The incubation periods were 8 hours for the detection of signaling proteins and 48 hours for the detection of ECM proteins.

Western Blotting

Total protein was extracted using radioimmunoprecipitation assay buffer (Thermo Fisher Scientific) with protease and phosphatase inhibitors (Sigma-Aldrich). Equal amounts of the proteins were resolved on 10% SDS-PAGE and transferred onto polyvinylidene fluoride membrane (MilliporeSigma, Burlington, MA, USA). The protein blots were analyzed with Pierce enhanced chemiluminescence western blotting substrate (Thermo Fisher Scientific). Images were captured using a UVP BioSpectrum 600 imaging system (Ultra-Violet Products Ltd., Cambridge, UK). The relative expressions of target proteins were evaluated by densitometry using ImageJ software (http://imagej.nih.gov/ij/index.html). Antibody information is provided in Supplementary Table S1.

RNA Isolation and Quantitative Real-Time PCR

For quantitative real-time PCR analysis, the fibroblasts were seeded and treated with AICAR and TGF-β1 as already described. After 24 hours of incubation, the cells were harvested and total RNA extracted using an RNeasy Mini Kit (QIAGEN, Hilden, Germany) according to the manufacturer's protocol. The quality and quantity of the RNA extracts were assessed by spectrophotometry. The RNA was reverse-transcribed to cDNA with LaboPass cDNA synthesis kit (Cosmo Genetech, Seoul, Korea) according to the manufacturer's protocol. Quantitative PCR was performed using primer pairs of target genes listed in Supplementary Table S2. The reaction was performed in a 10-μL reaction volume with the Applied Biosystems SYBR Green PCR Master Mix (Thermo Fisher Scientific).

Collagen Gel Matrix Contraction Assay

Cells were resuspended in serum-free DMEM at a concentration of 1.5×10^5 cells/mL; 400 μL of the cell suspension was mixed with 200 μL of type I collagen from a Gibco rat tail tendon solution (Thermo Fisher Scientific), and 5 μL of 1-N NaOH was added to neutralize the mixture. The gel solutions were added to 24-well plates (600 µL per well) and incubated at 37°C for 30 minutes to polymerize. Next, 600 µL of DMEM mixed with vehicle, 5-ng/mL TGF-β1, or 5-ng/mL TGF-β1 plus 1-mM AICAR, constituting the three different treatment regiments, were added to the gels. The gels were dissociated from the wells and incubated at 37°C and 5% CO_2 in a humidified incubator. Contraction images of gels were captured at different time points using a digital camera at a fixed distance. The degree of contraction was quantified by measuring the surface area using Image J software. The experiment was done in triplicate for each treatment group.

Animal Work

Healthy 8-week-old male BALB/C mice used in this study were kept under standard animal room conditions (temperature, 24°C ± 1°C; humidity, 50% ± 5%) for 1 week to acclimatize. After acclimatization, alkali burns were inflicted on the right eye of the mice, using the following protocol: First, the mice were randomly divided into four groups of six. They were then anesthetized with isoflurane followed by placement of 2-mm-diameter filter paper soaked with 2 μL of 0.1-N NaOH solution on the central cornea for 30 seconds to cause a grade I to II burn.[29] The eyes were thoroughly

washed with sterilized physiological saline. The mice were housed in plastic cages and fed a normal diet, with a 12-hour/12-hour light/dark cycle. Topical application of drugs was done 4× daily. Group 1 mice served as positive controls and were not treated with the test drugs. Group 2 mice were treated with 1-mM AICAR. Group 3 mice were treated with steroid (0.1% flumetholone; Santen Pharmaceutical, Osaka, Japan). Group 4 mice were treated with 1-mM AICAR and steroid. In order to prevent bacterial infection, all of the injured eyes were treated with a topical antibiotic (0.5% levofloxacin; Santen). The uninjured left eye corneas were used as negative controls. The mice were euthanized after 21 days by cervical dislocation after anesthesia with isoflurane. The central cornea, over a 3.0-mm^2 area, was scanned with the anterior segment 5 line raster method using CIRRUS HD-OCT (Carl Zeiss Meditec, Jena, Germany). The corneas were harvested and protein extracted for western blotting. Briefly, the tissues were excised and homogenized using TissueLyser II (QIAGEN) in a suitable lysis buffer—125-mM Tris-HCl, pH 7.0; 0.1% Triton X-100 (Sigma-Aldrich); 0.1% Tween 20 (Sigma-Aldrich); 100 mM NaCl; and 0.1% SDS—for optimal protein extraction as shown in a previous study.[30] The homogenate was centrifuged at $10,000 \times g$ for 5 minutes at 4°C, and the supernatant with the extracted protein was collected and stored at −20°C. Harvested cornea tissues were also fixed in 10% phosphate-buffered formalin for histopathological analysis.

Immunohistochemistry

Paraffin sections of the corneal tissues were deparaffinized, rehydrated, and analyzed by immunohistochemistry using monoclonal antibodies against α-smooth muscle actin (α-SMA) (1:500) and fibronectin (1:500) incubated overnight at 4°C. Biotinylated secondary antibody and streptavidin–biotin–peroxidase (1:200, incubated for 1 hour at 37°C) were used to detect the target proteins. The sections were counterstained with hematoxylin, dehydrated, and mounted.

Statistical Analysis

The data were analyzed using Prism 5.0 software (Graph-Pad, San Diego, CA, USA). Statistical comparisons were done using ANOVA, and post-test analysis was performed using Tukey's multiple comparison as appropriate. Statistical significance was defined as $P < 0.05$ in all cases.

RESULTS

AICAR Suppressed TGF-β1 and Extracellular Matrix Protein Accumulation in Corneal Fibroblasts Following Alkali Injury

To examine the possible mechanisms that may be involved in the antifibrotic effect of AICAR, we looked at TGF-β1 protein synthesis in response to alkali burn. Corneal tissues of mouse models of alkali burns, treated with or without AICAR, and uninjured control cornea tissues were analyzed by western blotting. Results showed that alkali injury caused a significant increase in TGF-β1 protein synthesis, which caused a corresponding significant increase in myofibroblast differentiation. Treatment with AICAR, however, resulted in a significant decrease in the TGF-β1 protein synthesis ($P = 0.0091$) (Fig. 1). The decreased TGF-β1 protein synthesis was seen to correspond also to a decreased myofibrob-

last differentiation and extracellular matrix (ECM) protein synthesis in the group treated with AICAR compared with the untreated group (α-SMA, $P = 0.0133$; fibronectin, $P = 0.0118$) (Fig. 1). Immunohistochemistry images of the mice corneal tissues also showed a marked decrease in the expression of fibronectin and α-SMA in the groups treated with AICAR compared with the untreated groups (Fig. 2).

OCT images of the mice cornea showed irregular epithelium and increased stroma thickness with high hyperreflectivity indicating excessive neovascularization and fibrosis in the untreated group. Conversely, mice treated with AICAR showed a more homogeneous, less hyperreflective, and more regular corneal thickness, indicating reduced ECM protein synthesis and confirming the western blotting results (Supplementary Figure Fig. S1).

Induction of fibrosis in vitro by directly treating cells with TGF-β1 also led to a marked increase in the expression of α-SMA, fibronectin, and the fibronectin EDA isoform (EDA-FN) compared with vehicle-treated control cells. AICAR pretreatment, however, significantly suppressed the expression of these proteins ($P = 0.0024$ for α-SMA and $P < 0.0001$ for fibronectin and EDA-FN) (Fig. 3A). The western blots were confirmed by real-time PCR results, which also showed a significantly decreased relative mRNA transcription of these proteins, as well as collagen 1 ($P = 0.0025$ for α-SMA; $P < 0.0001$ for fibronectin; $P = 0.0368$ for EDA-FN; $P = 0.0014$ for collagen 1) (Fig. 3B).

AICAR Suppressed Fibroblast Contraction

Collagen contractility is a characteristic of activated fibroblasts. To confirm the effect of AICAR on activated fibroblasts and subsequently on myofibroblast differentiation, the collagen gel matrix contraction assay was used. Our results showed AICAR suppressed fibroblast activation by TGF-β1. The cells treated with AICAR showed less contraction of the gel area compared with those treated with only TGF-β1 (Fig. 4). Although a slight difference in cell contraction was observed between the vehicle-treated controls and AICAR treated groups, it was not significant.

Anti-Fibrotic Effect of AICAR Is Dependent on AMPK Signaling

To investigate the molecular mechanism of AICAR in the inhibition of corneal fibrosis, we pretreated the primary human corneal fibroblasts with the AMPK-specific signaling inhibitor Compound C. First, we confirmed the activation of the AMPK signaling by AICAR. The result showed a significant increase in phosphorylated AMPK protein synthesis in the primary human corneal fibroblasts with TGF-β1 treatment ($P = 0.0007$). As shown in our results, Compound C treatment significantly blocked the antifibrotic effects of AICAR, depicted by the significantly high expression of α-SMA ($P = 0.0003$) and fibronectin ($P = 0.0041$) subsequent to the significantly suppressed AMPK signaling after TGF-β1 stimulation ($P < 0.0001$) (Fig. 5).

AICAR Suppressed Mammalian Target of Rapamycin Signaling

AMPK activation has been known to inhibit mammalian target of rapamycin (mTOR) signaling; thus, we studied the effects of AICAR on mTOR signaling in the corneal
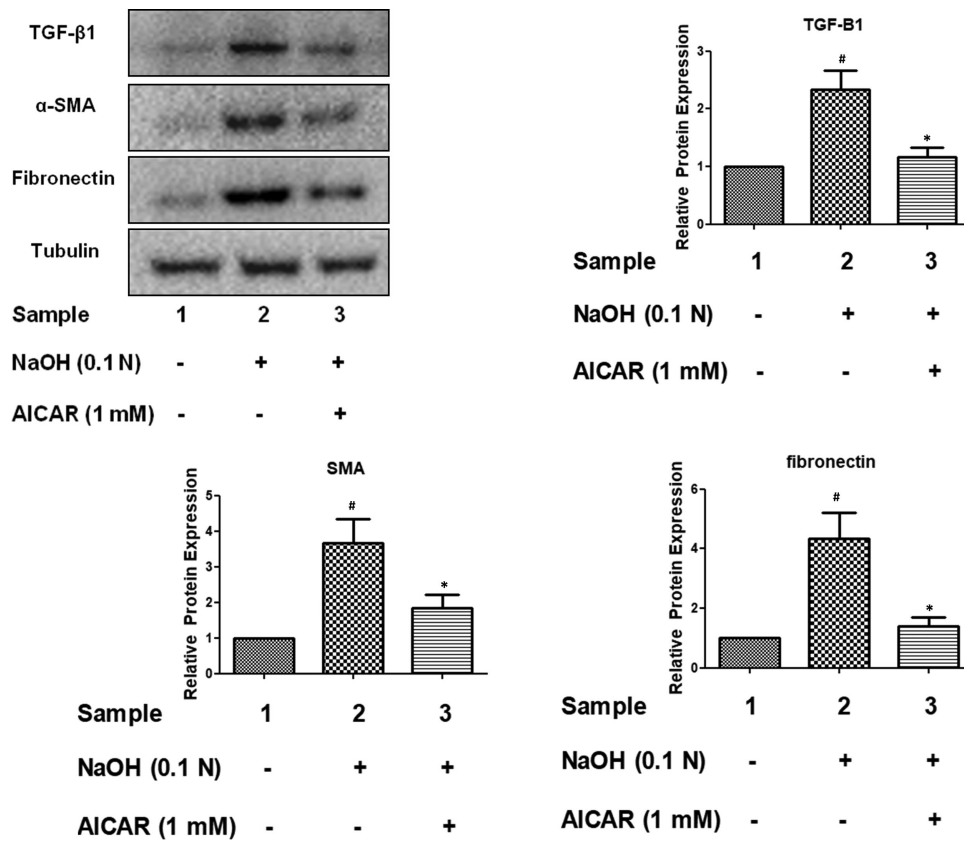
Figure 1. Effect of AICAR on alkali burn-induced ECM protein and TGF-β1 expression. Representative western blots and their quantitative analysis showing alkali burn-induced expression of TGF-β1, fibronectin, and α-SMA. AICAR treatment (1 mM) resulted in decreased expression of these proteins as shown. $^{\#}P < 0.05$ compared to vehicle-treated control cells; $^{*}P < 0.05$ compared to cells treated only with NaOH.
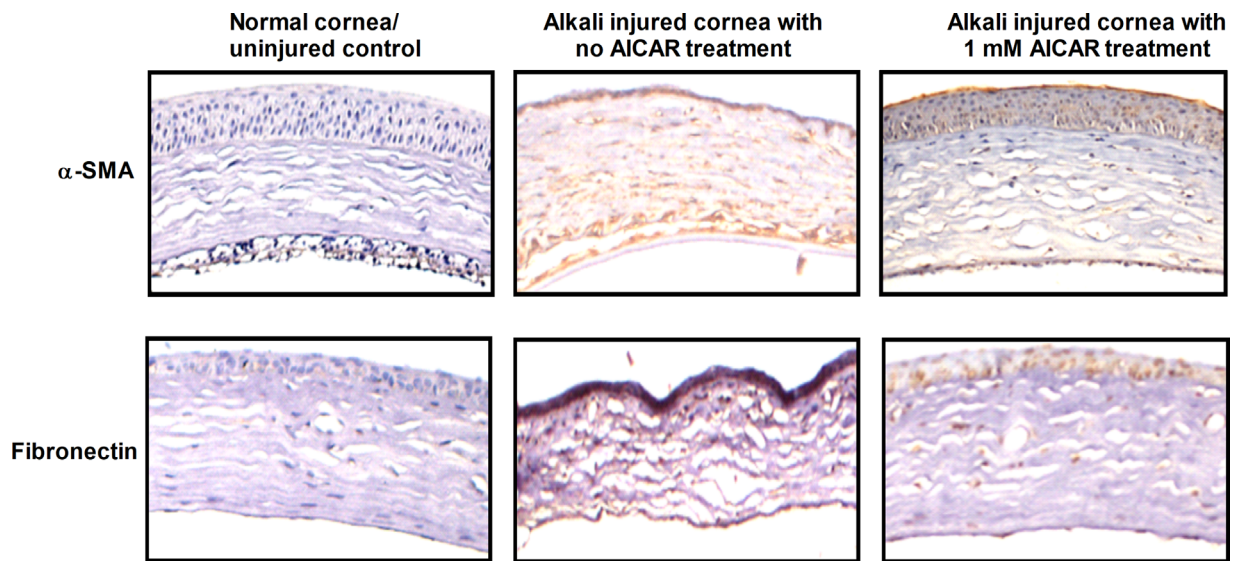

Figure 2. Immunohistochemistry images of mice cornea. Histopathological analysis of mice corneal tissues showing a marked decrease in the expression of fibronectin and α-SMA in the groups treated with AICAR compared with the untreated groups 3 weeks after alkali injury. Magnification is 200×.
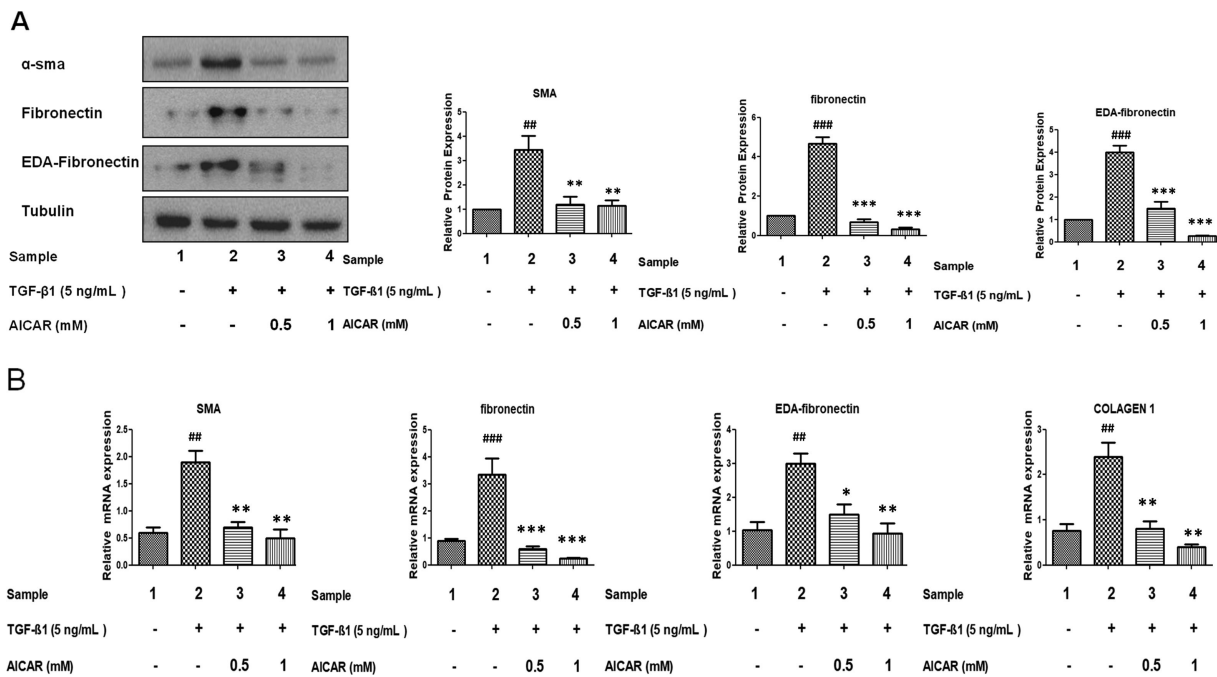
FIGURE 3. Effect of AICAR on TGF-β1-induced ECM protein expression and myofibroblast differentiation. (**A**) Representative western blots and their quantitative analysis showing a significant antifibrotic effect of AICAR on TGF-β1-induced expression of α-SMA, EDA-FN, and fibronectin. (**B**) Analysis of mRNA transcript levels also shows a significant antifibrotic effect of AICAR on TGF-β1-induced transcription of α-SMA, fibronectin, collagen, and EDA-FN. ##$P < 0.01$ and ###$P < 0.001$ compared to vehicle-treated control cells; *$P < 0.05$, **$P < 0.01$, and ***$P < 0.001$ compared to cells treated only with TGF-β1.

fibroblasts. The results indicated that AMPK activation by AICAR resulted in a correspondent significant decrease in phosphorylated mTOR ($P = 0.0004$) and phosphorylated p70S6K ($P = 0.0001$) expression, indicating mTOR signaling inhibition (Fig. 6).

DISCUSSION

Chemical injuries to the eye represent about 11.5% to 22.1% of all ocular traumas, with alkali substances being responsible for about 60% of these injuries.[31–33] These injuries present with very severe consequences due to the lipophilic nature of alkali, which enables them to penetrate the eye more deeply through saponification of membrane lipids. Severe damage to the corneal and conjunctival epithelium may cause damage to the pluripotent limbal stem cells, thus destroying their ability to regenerate and maintain the cornea. Alkali substances also denature the collagen matrix of the cornea, further penetrating into the corneal stroma.[2] The transparent nature of the cornea is important for its proper functioning; therefore, a normal healing response to a corneal injury involves events that work to retain its normal stromal structure and function. An abnormal healing response, however, leads to the loss of corneal transparency due to myofibroblast differentiation of the stromal keratocytes and fibrosis.[34,35] The opaque nature of these myofibroblasts is partly due to a reduced production of corneal crystallin and increased production of disorganized ECM proteins.[36,37] Our results confirm these previous findings, as they showed increased ECM protein synthesis and myofibroblast differentiation after alkali injury; however, treatment with AICAR suppressed these fibrotic responses significantly (Figures 1 to 4). The OCT images obtained also

showed less epithelial damage and reduced inflammation and corneal opacity (Supplementary Fig. S1) in the group treated with AICAR. We also examined the effectiveness of AICAR and 0.1% flumetholone as a combined therapy, as this steroid is used for suppressing inflammation and minimization scarring. Our OCT images showed much improvement in epithelial healing, significantly reduced corneal inflammation and opacity, and an overall improved appearance of the cornea compared to the groups treated with only AICAR or flumetholone (Supplementary Fig. S1). Further research into such combination therapies presents a great prospect to lowering dosage and application period of these steroids, thus minimizing their adverse effects, such as raised intraocular pressure, cataract, and suppression of immune response.[38]

The increased synthesis of TGF-β1 after corneal injury has been implicated in the development of ocular fibrosis in several studies.[39–45] TGF-β1 and its receptors are expressed in the epithelium and stromal layers of the cornea. It is known to have inhibitory effects on corneal epithelial cell proliferation,[46,47] while having stimulatory effects on stromal fibroblast proliferation.[48] Thus, its increased synthesis in the wounded area can lead to delayed re-epithelialization, increased fibroblast proliferation, increased extracellular matrix synthesis, and acceleration of myofibroblast differentiation. Our results showed a significant increase in the synthesis of TGF-β1 after alkali injury (Fig. 1). Research indicates that functional and structural defects in the epithelial basement membrane generated after corneal injury result in movement of TGF-β1 from the epithelium to the stroma.[49,50] This causes its receptor activation in these cells,[51] leading to downstream signaling events that result in myofibroblast differentiation of the otherwise relatively
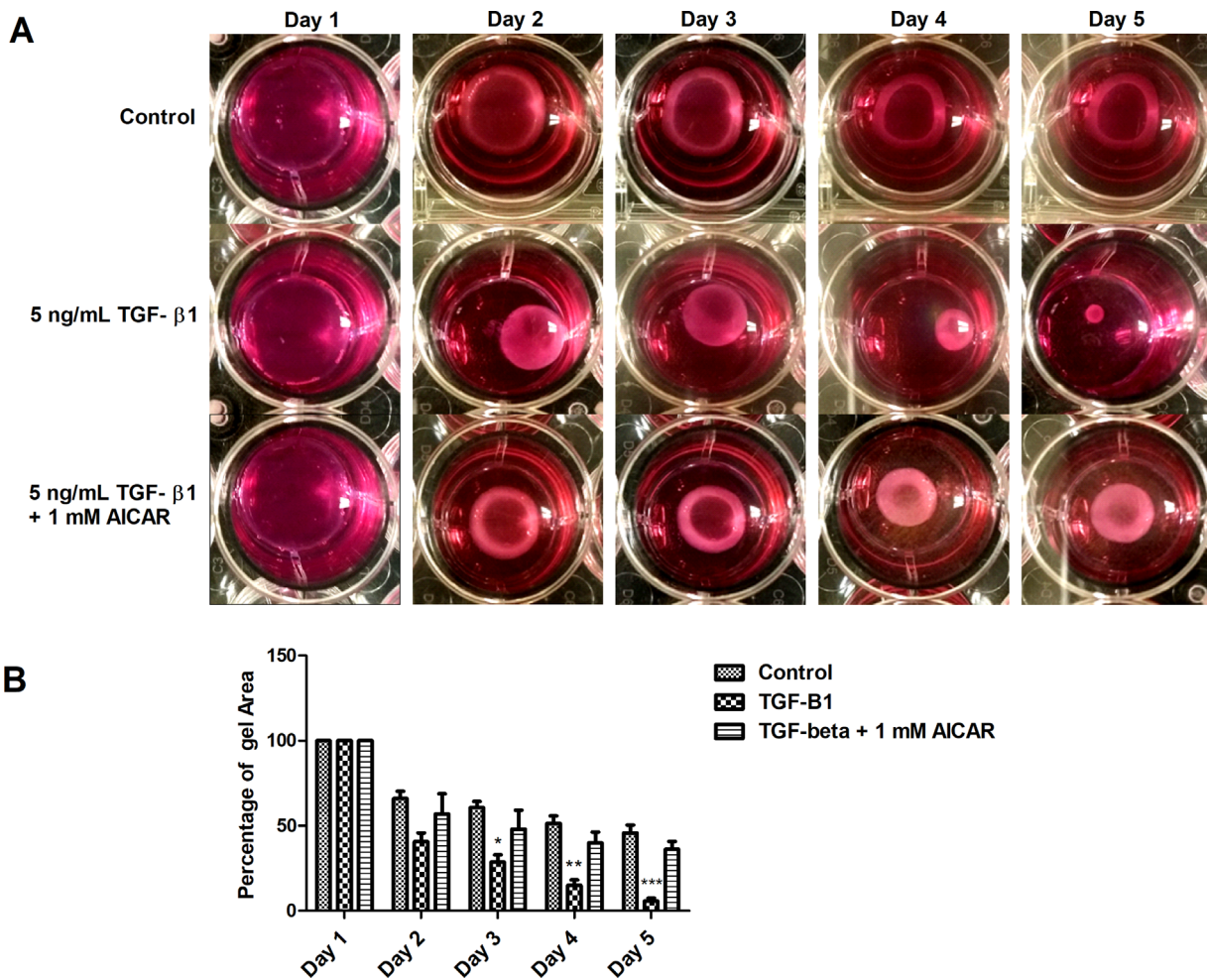
FIGURE 4. Collagen gel matrix contraction images. (**A**) Representative gel images and (**B**) the quantitative analysis of percentage gel area showed no significant difference in gel contraction between the vehicle-treated control cells and cells treated with TGF-β1 plus AICAR (1 mM) throughout the test period. However, the vehicle-treated control cells and cells treated only with TGF-β1 showed significant differences in gel contraction from test day 3. *$P < 0.05$, **$P < 0.01$, and ***$P < 0.001$ compared to vehicle-treated control cells.

quiescent keratocytes,[35,52] suppression of apoptosis in the myofibroblasts and their precursors,[53] their subsequent accumulation in the stroma, and a consequent corneal opacity. Because TGF-β1 has been shown to be required for corneal healing,[6–8] preventing the excessive activation of its receptors and not totally blocking its signaling in the corneal stroma upon epithelial injury could be an effective way of preventing fibrosis.

TGF-β1 overexpression induces VEGF and MCP-1 expression at the site of injury, leading to neovascularization and inflammation.[9,10] Although our work focused only on fibrosis or myofibroblast activation, AICAR has also been shown to suppress inflammation by inhibiting nuclear factor kappa B via AMPK-dependent and independent pathways,[54–56] as well as the AMPK-dependent activation of the protein deacetylase Sirt[57] in immune cells. Indeed, the systemic administration of AICAR and metformin, another pharmacological AMPK activator, in the treatment of type 2 diabetes mellitus and in wound healing is premised on their anti-inflammatory actions in addition to their major modes of action.[58–61] Taken together with our results, AICAR may be inhibiting alkali injury-induced cornea inflammation and accelerating corneal wound healing by reducing the production of angiogenic factors and inflammatory cytokines.

TGF-β1 also plays an important role in modulating ECM remodeling after injury by regulating the expression of matrix metalloproteinases (MMPs), which are proteinases involved in the degradation and removal of ECM from the tissues during repair. A dysregulated expression of MMPs, however, also activates TGF-β1 and stimulates myofibroblast differentiation, forming a bidirectional regulatory loop.[62] Because AICAR downregulated TGF-β1 protein synthesis in cornea fibroblasts, its effect on the expression of MMPs is an interesting area of further research.

Our investigations showed that AMPK activation was involved in the antifibrotic effect, as blocking of the AMPK pathway by Compound C attenuated the antifibrotic response. Studies on the effects of AICAR on mTOR signaling also showed that AMPK activation blocked the mTOR pathway. Other studies have found that mTOR signaling plays an important role in the TGF-β1-induced epithelial–mesenchymal transition,[63–66] which in turn plays a role in the origin of fibroblasts during organ fibrosis in adult tissues.[67] Our results showed that AICAR suppressed the upregulation of ECM proteins by inhibiting TGF-β1-induced
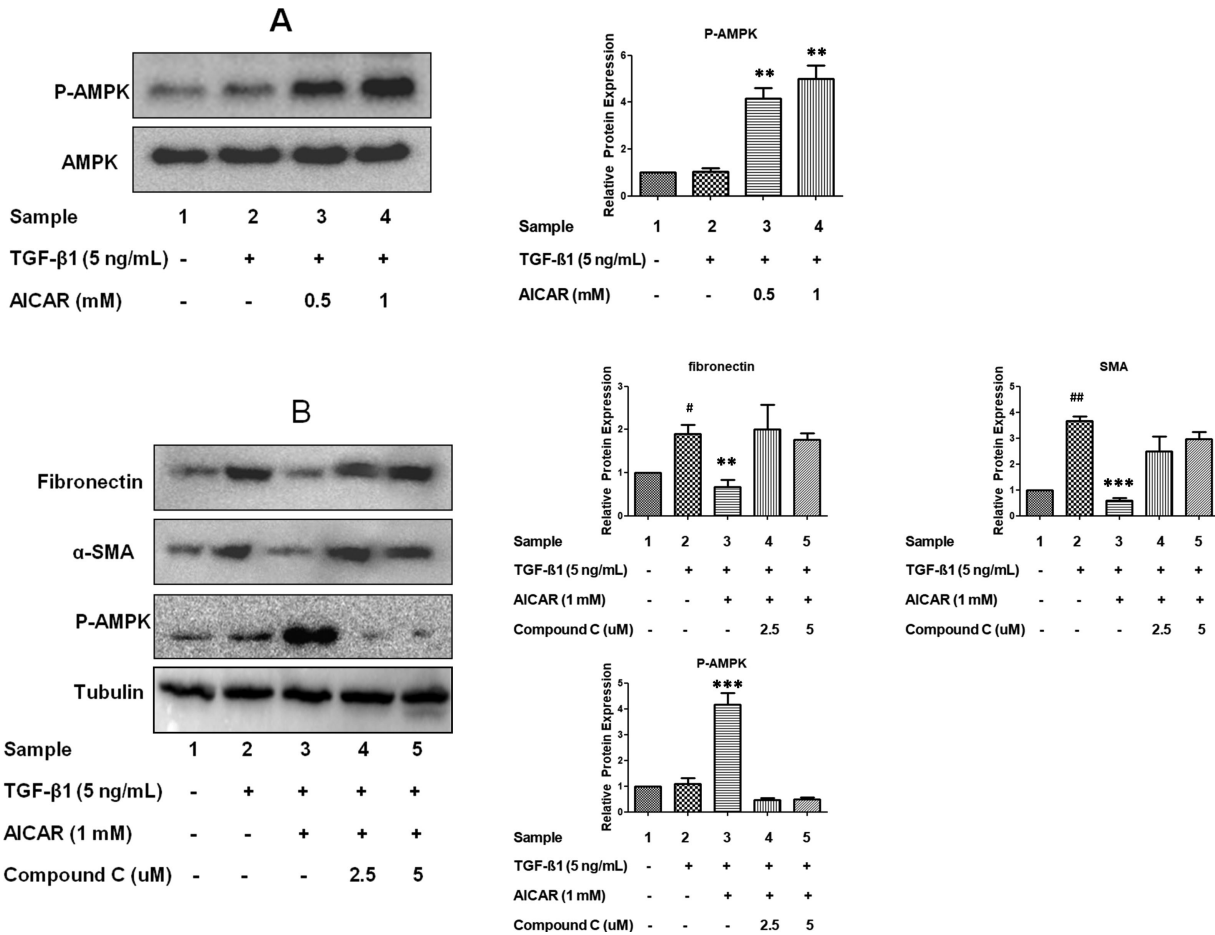
Figure 5. Effect of inhibition of AMPK signaling on the antifibrotic effect of AICAR. (**A**) Representative western blots and their quantitative analysis showed a significant increase in AMPK activation after AICAR treatment. (**B**) Blots also show that AICAR treatment caused a significant decrease in the TGF-β1-induced expression of α-SMA and fibronectin, which was countered by Compound C treatment subsequent to a significant decrease in AMPK level. $^{\#}P < 0.05$ and $^{\#\#}P < 0.01$ compared to vehicle-treated control cells; $^{**}P < 0.01$ and $^{***}P < 0.001$ compared to cells treated only with TGF-β1.
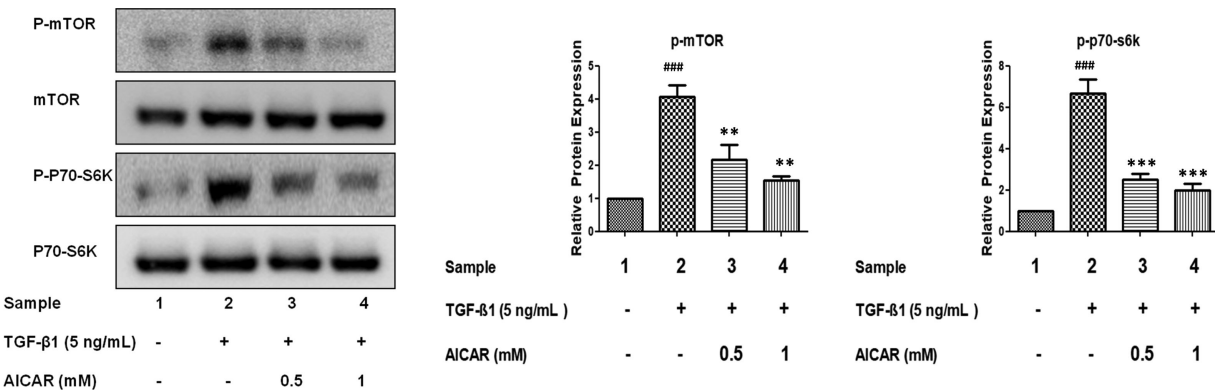

Figure 6. Effect of AICAR on mTOR signaling. Representative western blots of phosphorylated mTOR and phosphorylated p70S6K and their quantitative analysis showing the suppressive effect of AICAR on these signaling pathways after TGF-β1-induced signaling. $^{\#\#\#}P < 0.001$ compared to vehicle-treated control cells; $^{**}P < 0.01$ and $^{***}P < 0.001$ compared to cells treated only with TGF-β1.

mTOR–p70S6K signaling (Fig. 6). Previous studies have indicated activation of the mTOR pathway in ocular fibrosis,[68,69] and, not surprisingly, mTOR inhibitors have exhibited an antifibrotic effect in the corneal tissue.[68,70] Investigations into Smad and mitogen-activated protein kinase signaling, which are also downstream TGF-β1 signaling, showed that AICAR has no effect on these pathways in cornea fibroblasts (Supplementary Fig. S2).

In this study, we showed that activation of the mTORC1 pathway was involved in the fibrotic process that occurred subsequent to corneal alkali injury, mediated by TGF-β1. Furthermore, this study demonstrated that fibrosis induced by corneal alkali injury or TGF-β1 fibrosis could be treated by modulating the AMPK pathway, which is the upstream signal of the mTORC1 pathway. Taking into consideration the cytotoxicity of mTOR inhibitors, an AMPK agonist could be used with greater safety. Research also shows that a drug that specifically blocks myofibroblast differentiation from the precursor cells without adversely affecting other corneal cells would be the best way to inhibit fibrosis.[39] There is a great need to identify such drugs. AMPK activation therapies present a promising alternative adjuvant therapy.

Acknowledgments

Disclosure: **S.A. Nuwormegbe**, None; **S.W. Kim**, None

References

1. Fish R, Davidson RS. Management of ocular thermal and chemical injuries, including amniotic membrane therapy. *Curr Opin Ophthalmol*. 2010;21:317–321.

2. Singh P, Tyagi M, Kumar Y, Gupta KK, Sharma PD. Ocular chemical injuries and their management. *Oman J Ophthalmol*. 2013;6:83–86.

3. Tuft SJ, Shortt AJ. Surgical rehabilitation following severe ocular burns. *Eye (Lond)*. 2009;23:1966–1971.

4. Eslani M, Baradaran-Rafii A, Movahedan A, Djalilian AR. The ocular surface chemical burns. *J Ophthalmol*. 2014;2014:196827.

5. Saika S, Okada Y, Miyamoto T, et al. Role of p38 MAP kinase in regulation of cell migration and proliferation in healing corneal epithelium. *Invest Ophthalmol Vis Sci*. 2004;45:100–109.

6. Andresen JL, Ehlers N. Chemotaxis of human keratocytes is increased by platelet-derived growth factor-BB, epidermal growth factor, transforming growth factor-alpha, acidic fibroblast growth factor, insulin-like growth factor-I, and transforming growth factor-beta. *Curr Eye Res*. 1998;17:79–87.

7. You L, Kruse FE. Differential effect of activin A and BMP-7 on myofibroblast differentiation and the role of the Smad signaling pathway. *Invest Ophthalmol Vis Sci*. 2002;43:72–81.

8. Ashcroft GS, Yang X, Glick AB, et al. Mice lacking Smad3 show accelerated wound healing and an impaired local inflammatory response. *Nat Cell Biol*. 1999;1:260–266.

9. Nakagawa T, Li JH, Garcia G, et al. TGF-β induces proangiogenic and antiangiogenic factors via parallel but distinct Smad pathways. *Kidney Int*. 2004;66:605–613.

10. Abraham S, Sawaya BE, Safak M, Batuman O, Khalili K, Amini S. Regulation of MCP-1 gene transcription by Smads and HIV-1 Tat in human glial cells. *Virology*. 2003;309:196–202.

11. Ambati B, Nozaki M, Singh N, et al. Corneal avascularity is due to soluble VEGF receptor-1. *Nature*. 2006; 443:993–997.

12. Anderson C, Zhou Q, Wang S. An alkali-burn injury model of corneal neovascularization in the mouse. *J Vis Exp*. 2014;86:51159.

13. Tesch GH, Schwarting A, Kinoshita K, Lan HY, Rollins BJ, Kelley VR. Monocyte chemoattractant protein-1 promotes macrophage-mediated tubular injury, but not glomerular injury, in nephrotoxic serum nephritis. *J Clin Invest*. 1999;103:73–80.

14. Chong RS, Lee YS, Chu SWL, Toh LZ, Wong TTL. Inhibition of monocyte chemoattractant protein 1 prevents conjunctival fibrosis in an experimental model of glaucoma filtration surgery. *Invest Ophthalmol Vis Sci*. 2017;58:3432–3439.

15. Carling D. The AMP-activated protein kinase cascade–a unifying system for energy control. *Trends Biochem Sci*. 2004;29:18–24.

16. Hawley SA, Pan DA, Mustard KJ, et al. Calmodulin-dependent protein kinase kinase-beta is an alternative upstream kinase for AMP-activated protein kinase. *Cell Metab*. 2005;2:9–19.

17. Mihaylova MM, Shaw RJ. The AMPK signalling pathway coordinates cell growth, autophagy and metabolism. *Nat Cell Biol*. 2011;13:1016–1023.

18. Sabina RL, Patterson D, Holmes EW. 5-Amino-4-imidazolecarboxamide riboside (Z-riboside) metabolism in eukaryotic cells. *J Biol Chem*. 1985;260:6107–6114.

19. Bijland S, Mancini SJ, Salt IP. Role of AMP-activated protein kinase in adipose tissue metabolism and inflammation. *Clin Sci (Lond)*. 2013;124:491–507.

20. Srivastava RA, Pinkosky SL, Filippov S, et al. AMP activated protein kinase: an emerging drug target to regulate imbalances in lipid and carbohydrate metabolism to treat cardiometabolic diseases. *J Lipid Res*. 2012;53:2490–2514.

21. Garcia D, Shaw RJ. AMPK: mechanisms of cellular energy sensing and restoration of metabolic balance. *Mol Cell*. 2017;66:789–800.

22. O'Neill LA, Hardie DG. Metabolism of inflammation limited by AMPK and pseudo-starvation. *Nature*. 2013;493:346–355.

23. Lim JY, Oh MA, Kim WH, Sohn HY, Park SI. AMP-activated protein kinase inhibits TGF-β-induced fibrogenic responses of hepatic stellate cells by targeting transcriptional coactivator p300. *J Cell Physiol*. 2012;227:1081–1089.

24. Mishra R, Cool BL, Laderoute KR, Foretz M, Viollet B, Simonson MS. AMP-activated protein kinase inhibits transforming growth factor-beta-induced Smad3-dependent transcription and myofibroblast transdifferentiation. *J Biol Chem*. 2008;283:10461–10469.

25. Lempiainen J, Finckenberg P, Levijoki J, Mervaala E. AMPK activator AICAR ameliorates ischaemia reperfusion injury in the rat kidney. *Br J Pharmacol*. 2012;166:1905–1915.

26. Satriano J, Sharma K, Blantz RC, Deng A. Induction of AMPK activity corrects early pathophysiological alterations in the subtotal nephrectomy model of chronic kidney disease. *Am J Physiol Renal Physiol*. 2013;305:F727–F733.

27. Myerburg MM, King JD, Oyster NM, et al. AMPK agonists ameliorate sodium and fluid transport and inflammation in cystic fibrosis airway epithelial cells. *Am J Respir Cell Mol Biol*. 2010;42:676–684.

28. Jester JV, Huang J, Fisher S, et al. Myofibroblast differentiation of normal human keratocytes and hTERT, extended-life human corneal fibroblasts. *Invest Ophthalmol Vis Sci*. 2003;44:1850–1858.

29. Bai JQ, Qin HF, Zhao SH. Research on mouse model of grade II corneal alkali burn. *Int J Ophthalmol*. 2016;9:487–490.

30. Patel N, Solanki E, Picciani R, Cavett V, Caldwell-Busby JA, Bhattacharya SK. Strategies to recover proteins from ocular tissues for proteomics. *Proteomics*. 2008;8:1055–1070.

31. Clare G, Suleman H, Bunce C, Dua H. Amniotic membrane transplantation for acute ocular burns. *Cochrane Database Syst Rev*. 2012;9:CD009379.

32. Wagoner MD. Chemical injuries of the eye: current concepts in pathophysiology and therapy. *Surv Ophthalmol*. 1997;41:275–313.

33. Colby K. Chemical injuries of the cornea. *Focal Points Am Acad Ophthalmol*. 2010;28:1–14.

34. Wilson SE. Corneal myofibroblast biology and pathobiology: generation, persistence, and transparency. *Exp Eye Res*. 2012;99:78–88.

35. Torricelli AA, Santhanam A, Wu J, Singh V, Wilson SE. The corneal fibrosis response to epithelial-stromal injury. *Exp Eye Res*. 2016;142:110–118.

36. Jester JV. Corneal crystallins and the development of cellular transparency. *Semin Cell Dev Biol*. 2008;19:82–93.

37. Jester JV, Moller-Pedersen T, Huang J, et al. The cellular basis of corneal transparency: evidence for 'corneal crystallins'. *J Cell Sci*. 1999;112:613–622.

38. Mills DW, Oliver GL. Corticosteroid glaucoma. *Can Med Assoc J*. 1965; 92:1084–1085.

39. Nuwormegbe SA, Sohn JH, Kim SW. A PPAR-gamma agonist rosiglitazone suppresses fibrotic response in human pterygium fibroblasts by modulating the p38 MAPK pathway. *Invest Ophthalmol Vis Sci*. 2017;58:5217–5226.

40. Zhang H, Liu ZL. Transforming growth factor-β neutralizing antibodies inhibit subretinal fibrosis in a mouse model. *Int J Ophthalmol*. 2012;5:307–311.

41. Saika S. TGFbeta pathobiology in the eye. *Lab Invest*. 2006;86:106–115.

42. Stahnke T, Kowtharapu BS, Stachs O, et al. Suppression of TGF-β pathway by pirfenidone decreases extracellular matrix deposition in ocular fibroblasts in vitro. *PLoS One*. 2017;12:e0172592.

43. Sumioka T, Ikeda K, Okada Y, Yamanaka O, Kitano A, Saika S. Inhibitory effect of blocking TGF-beta/Smad signal on injury-induced fibrosis of corneal endothelium. *Mol Vis*. 2008;14:2272–2281.

44. Saika S, Yamanaka O, Sumioka T, et al. Fibrotic disorders in the eye: targets of gene therapy. *Prog Retin Eye Res*. 2008;27:177–196.

45. Branton MH, Kopp JB. TGF-β and fibrosis. *Microbes Infect*. 1999;1:1349–1365.

46. Pancholi S, Tullo A, Khaliq A, Foreman D, Boulton M. The effects of growth factors and conditioned media on the proliferation of human corneal epithelial cells and keratocytes. *Graefes Arch Clin Exp Ophthalmol*. 1998;236:1–8.

47. Haber M, Cao Z, Panjwani N, Bedenice D, Li WW, Provost PJ. Effects of growth factors (EGF, PDGF-BB and TGF-beta 1) on cultured equine epithelial cells and keratocytes: implications for wound healing. *Vet Ophthalmol*. 2003;6:211–217.

48. Andresen JL, Ledet T, Ehlers N. Keratocyte migration and peptide growth factors: the effect of PDGF, bFGF, EGF, IGF-I, aFGF and TGF-β on human keratocyte migration in a collagen gel. *Curr Eye Res*. 1997;16:605–613.

49. Wilson SE, Liu JJ, Mohan RR. Stromal–epithelial interactions in the cornea. *Prog Retin Eye Res*. 1999;18:293–309.

50. Fini ME, Stramer BM. How the cornea heals: cornea-specific repair mechanisms affecting surgical outcomes. *Cornea*. 2005;24(suppl 8):S2–S11.

51. Kaur H, Chaurasia SS, Agrawal V, Suto C, Wilson SE. Corneal myofibroblast viability: opposing effects of IL-1 and TGF beta1. *Exp Eye Res*. 2009;89:152–158.

52. Jester JV, Huang J, Petroll WM, Cavanagh HD. TGFbeta induced myofibroblast differentiation of rabbit keratocytes requires synergistic TGFbeta, PDGF and integrin signaling. *Exp Eye Res*. 2002;75:645–657.

53. Barbosa FL, Chaurasia SS, Kaur H, de Medeiros FW, Agrawal V, Wilson SE. Stromal interleukin-1 expression in the cornea after haze-associated injury. *Exp Eye Res*. 2010;91:456.

54. Kirchner J, Brüne B, Namgaladze D. AICAR inhibits NFκB DNA binding independently of AMPK to attenuate LPS-triggered inflammatory responses in human macrophages. *Sci Rep*. 2018;8:7801.

55. Jhun BS, Jin Q, Oh YT, et al. 5-Aminoimidazole-4-carboxamide riboside suppresses lipopolysaccharide-induced TNF-alpha production through inhibition of phosphatidylinositol 3-kinase/Akt activation in RAW 264.7 murine macrophages. *Biochem Biophys Res Commun*. 2004;318:372–380.

56. Kuo CL, Ho FM, Chang MY, Prakash E, Lin WW. Inhibition of lipopolysaccharide-induced inducible nitric oxide synthase and cyclooxygenase-2 gene expression by 5-aminoimidazole-4-carboxamide riboside is independent of AMP-activated protein kinase. *J Cell Biochem*. 2008;103:931–940.

57. Yang Z, Kahn BB, Shi H, Xue BZ. Macrophage alpha1 AMP-activated protein kinase (alpha1AMPK) antagonizes fatty acid-induced inflammation through SIRT1. *J Biol Chem*. 2010;285:19051–19059.

58. Day EA, Ford RJ, Steinberg GR. AMPK as a therapeutic target for treating metabolic diseases. *Trends Endocrinol Metab*. 2017;28:545–560.

59. Hasanpour Dehkordi A, Abbaszadeh A, Mir S, Hasanvand A. Metformin and its anti-inflammatory and anti-oxidative effects; new concepts. *J Renal Inj Prev*. 2019;8:54–61.

60. Han X, Tao Y, Deng Y, Yu J, Sun Y, Jiang G. Metformin accelerates wound healing in type 2 diabetic db/db mice. *Mol Med Rep*. 2017;16:8691–8698.

61. Wang XR, Zhang MW, Chen DD, Zhang Y, Chen AF. AMP-activated protein kinase rescues the angiogenic functions of endothelial progenitor cells via manganese superoxide dismutase induction in type 1 diabetes. *Am J Physiol Endocrinol Metab*. 2011;300:E1135–E1145.

62. Jabłońska-Trypuć A, Matejczyk M, Rosochacki S. Matrix metalloproteinases (MMPs), the main extracellular matrix (ECM) enzymes in collagen degradation, as a target for anti-cancer drugs. *J Enzyme Inhib Med Chem*. 2016;31:177–183.

63. Woodcock H, Peace S, Nanthakumar C, Maher T, Mercer P, Chamers R. mTOR signalling is an essential pathway for TGF-β1 induced collagen synthesis. *Eur Respir J*. 2015;46:PA935.

64. Zhai XX, Tang ZM, Ding JC, Lu XL. Expression of TGF-β1/mTOR signaling pathway in pathological scar fibroblasts. *Mol Med Rep*. 2017;15:3467–3472.

65. Lamouille S, Connolly E, Smyth JW, Akhurst RJ, Derynck R. TGF-β-induced activation of mTOR complex 2 drives epithelial-mesenchymal transition and cell invasion. *J Cell Sci*. 2012;125:1259–1273.

66. Cheng KY, Hao M. Mammalian target of rapamycin (mTOR) regulates transforming growth factor-β1 (TGF-β1)-induced epithelial-mesenchymal transition via decreased pyruvate kinase M2 (PKM2) expression in cervical cancer cells. *Med Sci Monit*. 2017;23:2017–2028.

67. Kalluri R, Neilson EG. Epithelial-mesenchymal transition and its implications for fibrosis. *J Clin Invest*. 2003;112:1776–1784.

68. Yousefimilani F, Milani B, Sagha H, Djalilian A. Rapamycin helps to maintain colony forming efficiency in corneal epithelial cells. *Invest Ophthalmol Vis Sci*. 2013;54:555.

69. Kim SW, Kim HI, Thapa B, Nuwormegbe S, Lee K. Critical role of mTORC2-Akt signaling in TGF-β1-induced myofibroblast differentiation of human pterygium fibroblasts. *Invest Ophthalmol Vis Sci*. 2019;60:82–92.

70. Shin YJ, Hyon JY, Choi WS, et al. Chemical injury-induced corneal opacity and neovascularization reduced by rapamycin via TGF-β1/ERK pathways regulation. *Invest Ophthalmol Vis Sci*. 2013;54:4452–4458.

Investigative Ophthalmology & Visual Science